文章编号: 1001－2060(2003)01－0050－04

薄层毛细多孔介质湿区干燥过程相变传热传质常压模型

卢　涛, 沈胜强
(大连理工大学 动力工程系, 辽宁 大连　116024)

摘　要: 对液相残余饱和度 S_{ir} 作了一个定义, 把含湿毛细多孔介质干燥区域分为湿区和干区。建立了以液相饱和度 S 和温度 T 为参数的湿区干燥过程相变传热传质常压模型。采用全隐式有限差分方法对模型进行了数值计算。数值解表明, 模型能很好地预测湿区干燥过程中的液相饱和度 S 和温度 T 的变化。

关　键　词: 毛细多孔介质; 相变; 传热传质

中图分类号: TK124　　文献标识码: A

1　引　言

毛细多孔介质相变传热传质是自然界和工业生产过程中普遍存在的现象。能源、环境、地质、材料、化工、生物、农业等许多领域都涉及到多孔介质相变传热传质问题。不存在化学反应时, 多孔介质内部传热传质的主导驱动势为: 压力梯度、浓度梯度、温度梯度。毛细现象是毛细多孔介质的重要特征, 对传热传质起重要作用。流体在一定条件下要发生相变, 如蒸发和凝结, 使得整个传热传质行为更为复杂。

建立多孔介质传热传质数学模型的主要理论大体上分为 Luikov 唯象理论和 Whitaker 体积平均理论, 前者控制方程的唯象系数难于确定, 后者的控制方程呈现高度非线性而不易求解和应用[1]。有学者指出, 毛细多孔介质的传热传质不是由扩散而是由毛细行为决定的[2]。毛细流不但会引起质量的迁徙, 而且会引起能量的传递。毛细多孔介质中的传热传质之间必然存在直接关系[3], 这种关系还在于浓度梯度和温度梯度的驱动[4]。多孔介质中的流体相变, 进一步加强了这种关系。因此, 毛细多孔介质相变传热传质是一相互耦合过程。

2　薄层毛细多孔介质干燥过程相变传热传质分析

设薄层毛细多孔介质上边界为对流边界, 下边界为绝热绝湿边界, 在干燥过程中, 介质和周围环境之间进行质量和能量的交换。液相蒸发使得液相质量减少, 蒸汽通过上边界向周围环境传递, 从而使介质的湿份不断减少; 同时, 液相蒸发需要吸收大量的蒸发潜热, 介质必然要和外界发生热交换, 以达到新的能量平衡。在干燥初期, 大量的蒸汽通过上边界向外蒸发, 随着干燥过程的进行, 上边界上的液相饱和度将越来越小, 将出现干点, 并在该边界上长大, 进而形成"蒸发界面"蒸发, 但此时介质内部孔隙中液相仍然保持连续相。当干点不再长大时, 蒸发界面逐渐向介质内部"入侵", 此时介质内部孔隙中的液相连续相将逐渐被"液岛"的形式所代替。定义蒸发界面边界上的液相饱和度为残余饱和度 S_{ir}, 通过分子热运动液相不能摆脱分子表面力的束缚而保持液相质量不变, 此时残余饱和度将保持不变。这样, 把 $S_{ir}<S<S_{cr}$ 的区域称为湿区, 把 $S=S_{ir}$ 的区域称为干区。S 为液相饱和度, S_{cr} 为临界饱和度。本文作者针对湿区干燥过程中的相变传热传质进行分析。

2.1　薄层毛细多孔介质湿区干燥过程相变传热传质常压模型数学描述

按照文献[5]介绍, 湿区混合气相压力基本保持不变, 对薄层毛细多孔介质湿区干燥过程相变传热传质作如下假设:

(1) 介质是一结构均匀的刚性连续介质, 其所属的物理属性都具有"体积平均"意义。

(2) 介质中的任意质点处于局部热力学平衡。

收稿日期: 2002－01－24; 修订日期: 2002－03－20

作者简介: 卢　涛(1975－), 男, 江西丰城人, 大连理工大学博士研究生.

(3) 蒸汽压符合 Clausius-Clapeyron 方程[5], 且混合气相压力保持常压。

(4) 流体遵循达西定律, 对液相考虑重力效应, 而忽略气相重力效应和分子扩散效应。

(5) 毛细力为温度和饱和度的函数, 符合 Leverett 关系式[5]。

2.1.1　质量守恒方程

在多孔介质内部, 由于蒸汽质量远远小于液相质量, 忽略蒸汽质量来定义液相饱和度[6]:

$$S = \frac{\varphi_l}{\varphi} \tag{1}$$

固相、液相和气相的体积分数分别为:

$\varphi_s = 1 - \varphi$, $\varphi_l = \varphi S$, $\varphi_g = \varphi(1 - S)$。

固相、液相和蒸汽相的相密度分别为:

$m_s = \rho_s \varphi_s = \rho_s(1 - \varphi)$, $m_l = \rho_l \varphi_l = \rho_l \varphi S$, $m_v = \rho_v \varphi(1 - S)$。

对液相和蒸汽相运用质量守恒定律:

$$\frac{\partial m_l}{\partial \tau} + \nabla \cdot (m_l u_l) = \delta \tag{2}$$

$$\frac{\partial m_v}{\partial \tau} + \nabla \cdot (m_v u_v) = -\delta \tag{3}$$

式中: φ、m、ρ、τ、u、δ 分别表示体积分数(或孔隙率)、相密度、密度、时间、速度和相变源项, 下标 l、s、v、分别表示液相、固相和蒸汽。

2.1.2　动量守恒方程

在薄层毛细多孔介质湿区干燥相变传热传质过程中, 由于流体的速度非常小, 用达西定律来表达动量方程。对于液相和蒸汽相分别为:

$$u_l = -\frac{k_l K}{\mu_l \varphi_l}(\nabla \cdot p_l + \rho_l g) = -\frac{k_l K}{\mu_l \varphi_l}[\nabla \cdot (p_g - p_c) + \rho_l g] \tag{4}$$

$$u_v = -\frac{k_v K}{\mu_v \varphi_v} \nabla \cdot p_v \tag{5}$$

式中: k、K、μ、p、g 分别表示相对渗透系数、绝对渗透系数、动力粘度、压力和重力加速度。

2.1.3　能量守恒方程

根据基本假设, 混合气体处于拟静止状态, 忽略粘性耗散, 能量守恒方程式如下:

$$\rho_p c_p \frac{\partial T}{\partial \tau} + (m_l u_l c_l) \nabla \cdot T = \nabla(\lambda_p \nabla T) + \delta h_{vap} \tag{6}$$

式中: c、λ、T 和 h_{vap} 分别表示定压比容、导热系数、温度和潜热, 下标 p 表示多孔介质。

2.2　薄层毛细多孔介质湿区干燥过程相变传热传质一维常压模型

对于一维常压模型, $x = 0$ 处, 下边界为不可渗透绝热边界:

$$m_l u_l + m_v u_v = 0 \tag{7}$$

$$\lambda_p \frac{\partial T}{\partial x} + m_l u_l h_{vap} = 0 \tag{8}$$

$x = L$ 处, 上边界给定传质传热边界:

$$m_l u_l + m_v u_v = k_m(\rho_v - \rho_0) \tag{9}$$

$$\lambda_p = \frac{\partial T}{\partial x} + m_l u_l h_{vap} = k_T(T_0 - T) \tag{10}$$

式中: x 为铅垂方向, 下标 0 表示外环境。

运用上述及相关热力学关系式, 方程式(2) 和式(3) 相加得到

$$S_S \frac{\partial S}{\partial \tau} + S_T \frac{\partial T}{\partial \tau} = \frac{\partial}{\partial x}\left[K_{SS} \frac{\partial S}{\partial x} + K_{ST} \frac{\partial T}{\partial x} + K_{SR}\right] \tag{11}$$

能量方程式(6) 可以写成

$$T_S \frac{\partial S}{\partial \tau} + T_T \frac{\partial T}{\partial \tau} = \frac{\partial}{\partial x}\left(\lambda_p \frac{\partial T}{\partial x}\right) - h_{vap} \frac{\partial}{\partial x}\left[K_{SS} \frac{\partial S}{\partial x} + K_{ST1} \frac{\partial T}{\partial x} + K_{SR}\right] + c_l\left(K_{SS} \frac{\partial S}{\partial x} + K_{ST1} \frac{\partial T}{\partial x} + K_{SR}\right) \frac{\partial T}{\partial x} \tag{12}$$

相应的边界条件为:

$$K_{SS} \frac{\partial S}{\partial x} + K_{ST} \frac{\partial T}{\partial x} + K_{SR} = 0 \tag{13}$$

$$\lambda_p \frac{\partial T}{\partial x} - h_{vap}\left(K_{SS} \frac{\partial S}{\partial x} + K_{ST1} \frac{\partial T}{\partial x} + K_{SR}\right) = 0 \tag{14}$$

$$-\left(K_{SS} \frac{\partial S}{\partial x} + K_{ST1} \frac{\partial T}{\partial x} + K_{SR}\right) = \frac{k_m M_v}{R}\left(\frac{p_v}{T} - \frac{p_{v0}}{T_0}\right) \tag{15}$$

$$\lambda_p \frac{\partial T}{\partial x} - h_{vap}\left(K_{SS} \frac{\partial S}{\partial x} + K_{ST1} \frac{\partial T}{\partial x} + K_{SR}\right) = k_T(T_0 - T) \tag{16}$$

式(11) ~式(16)中的各系数均可以表示成 S 或 T 的函数。

初始条件为:

$$T(x, \tau) = T_{ini} \tag{17}$$

$$p_g = p_0 \tag{18}$$

根据流体静力学, 有

$$\frac{\partial p_c}{\partial x} = -\rho_l g \tag{19}$$

3　一维常压模型的数值解

方程式(11) 和式(12) 及其边界条件和初始条件所构成的方程组是一个非线性定解问题, 采用全隐式有限差分方法来生成模型的代数方程组。能量

方程中的对流项采用迎风格式，其它各项采用中心差分。

对某一薄层含湿毛细多孔介质的干燥过程进行数值模拟，假设其基本干燥条件如下：初始温度 320.15 K，初始压力 $1.013\ 3\times 10^5$ Pa，介质厚度 0.01 m，外表面液相饱和度 0.9，残余饱和度为 0.1，环境温度 360 K，环境中蒸汽分压力为 2.5×10^3 Pa，上边界传质系数 0.014 m/s，上边界传热系数 15 W/(m^2 · K)。求解上述模型，得到了其干燥过程各参数的变化规律。

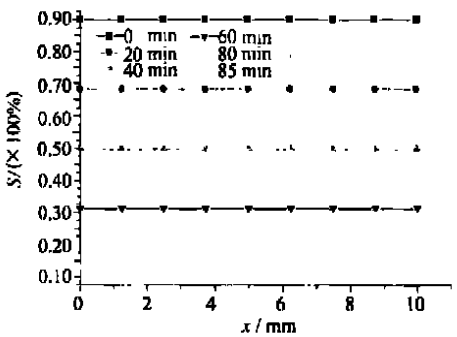

图 1 不同时间不同厚度饱和度分析

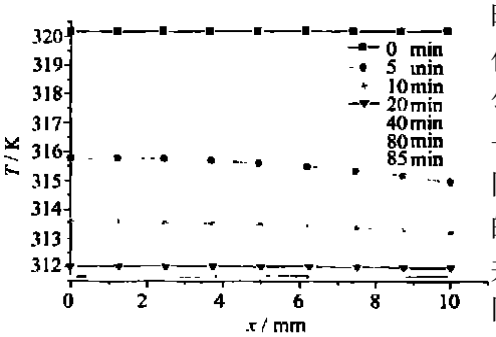

图 2 不同时间不同厚度温度分布

图 1 和图 2 分别给出了不同时刻多孔介质内饱和度和温度沿厚度方向的分布。在图 1 中，饱和度随时间的变化比较均匀，但同一时刻不同厚度上的饱和度并不相同，如图 3 和图 4 分别表示了第 20 min 和第 80 min 时饱和度分布，可以看出在干燥初期液相向上边界迁徙，这种迁徙是由于毛细势、渗流和蒸发凝结等机理共同作用的结果，一方面上边界处的饱和度大于下边界处的饱和度，这有利于蒸发过程；另一方面下边界处的蒸汽在向外输运的过程中所受到的阻碍较上边界处的蒸汽大，并在途中有部分蒸汽发生凝结，从而抑制蒸发过程，但有利于上边界蒸发及时得到液相补充。随着干燥过程的进行，这种饱和度分布趋势逐渐转向平坦，最后出现下边界处的饱和度大于上边界处的饱和度，如图 4 所示，在干燥末期，上边界处的液相饱和度相对较小，使得整个干燥过程减慢。图 2 描述了不同厚度处的温度在不同时间的分布，在前 20 min 内，温度的下降比较快，随后温度的变化不大。图 5 和图 6 分别表示了第 20 min 和第 80 min 时温度分布情况。可以看出，在干燥初期，由于上边界处蒸发凝结之净潜热量大于从外界导入的热量与对流传热之净量，所以上边界上温度略低，而在下边界处，这种关系趋于平衡；到了干燥末期，随着上边界蒸发速率的下降，蒸发所带走的热量相应变小，而外界向多孔介质内部导入热量与对流传热之净量相对于蒸发凝结之净潜热有盈余，使得在

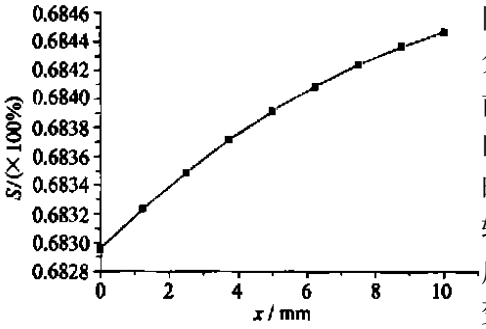

图 3 第 20 min 不同厚度上的饱和度

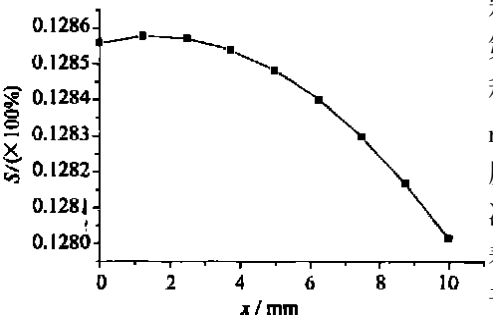

图 4 第 80 min 不同位置上的饱和度

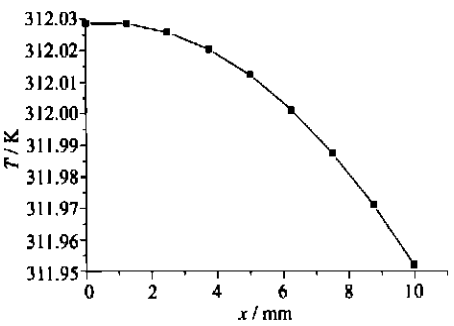

图 5 第 20 min 不同位置上的温度

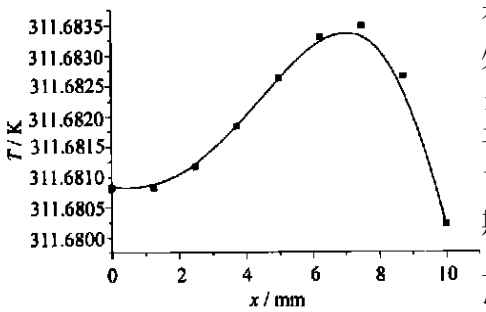

图 6 第 80 min 不同位置上的温度

(下转第 77 页)

面反映它对自然环境的影响。粉尘的危害主要是粉尘中的有害物质（如微量重金属元素、多环化合物等）的化学反应、粉尘对人体呼吸器官的损害以及对太阳辐射的吸收与散射，用㶲的概念对其进行分析时一方面需要更为精确地确定粉尘的物质构成，另一方面需要对㶲的定量计算进行深入的研究。

5　结论

本文应用㶲的概念对 PFBC－CC 系统的环境影响进行了初步分析，结果表明系统排放的 CO_2 和热量对环境的影响是不可忽略的；通过对 SO_2 和 $CaSO_4$ 的㶲分析表明，S 从 SO_2 转移到 $CaSO_4$ 可大大降低系统的环境影响。由于在模型建立和计算分析中人为因素和政策法规因素很小甚至没有，因此应用㶲方法分析系统的环境影响是一个比较客观的非货币化评价方法。在分析过程中可以看出，应用㶲方法分析环境影响问题时，参考环境模型建立得越完善，环境排放物的构成知道得越详尽，得到的分析结果就越全面可靠，在这方面还需要综合应用现代热力学、燃烧学、环境等学科的知识进行深入的研究和探讨。

参考文献：

[1] MARC A ROSEN, IBRAHIM DINCER. Exergy analysis of waste emissions[J]. **International Journal Energy Research**, 1999, **23**: 1159－1163.

[2] ROBERT U AYRES, LESLIE W AYRES. Katanlin martinas, exergy, waste accounting, and life-cycle analysis[J]. **Energy**, 1998, **25**(5): 355－363.

[3] MAKARYTCHEV S V. Environmental impact analysis of ACFB-based gas and power cogeneration[J]. **Energy**, 1998, **23**(9): 711－717.

[4] PETER MICHANELIS, TIM JACKSON, ROLAND CLIFT. Exergy analysis of the life cycle of steel[J]. **Energy**, 1998, **23**(3): 213－220.

[5] 朱明善. 能量的㶲分析[M]. 北京：清华大学出版社，1988.

（辉　编辑）

（上接第 52 页）

靠近上边界的地方，出现温度峰值。总体上，饱和度的变化总趋势是减少的，干燥初期液相向上边界迁徙，而到了末期，下边界处的饱和度高于上边界处的饱和度；对于温度，要受相变和传热平衡关系的制约，表现在干燥前期温度下降较快，随后变化略有波动。

4　结论

通过对薄层毛细多孔介质湿区干燥过程相变传热传质机理分析，建立了常压数学模型，该数学模型是以多孔介质液相饱和度 S 和温度 T 为参数的非线性偏微分方程组。采用全隐式有限差分方法对上述方程组进行了数值模拟，预测了液相饱和度 S 和温度 T 两参数的复杂变化，这种变化是受毛细、渗流、蒸发凝结和传热等机理共同作用的。模拟结果能较好地解释薄层毛细多孔介质干燥过程中的相变传热传质现象。

参考文献：

[1] ZHAO HUI WANG, GUOHUA CHEN. Heat and mass transfer during low intensity convection drying[J]. **Chemical Engineering Science**, 1999, **54**(17): 3899－3908.

[2] HUANG C L D, SIANG H H, BEST C H. Heat and moisture transfer in concrete slabs[J]. **Int J Heat Mass Transfer**, 1979, **22**(2): 257－266.

[3] LUIKOV A V. Systems of differential equations of heat and mass transfer in capillary-porous bodies (review)[J]. **Int J Heat Mass Transfer**, 1975, **18**(1): 1－14.

[4] HUANG C L D. Multi-phase moisture transfer in porous media subjected to temperature gradient[J]. **Int J Heat Mass Transfer**, 1979, **22**(9): 1295－1307.

[5] ILIC M, TURNER I W. Convective drying of a consolidated slab of wet porous material[J]. **Int J Heat Mass Transfer**, 1989, **32**(2): 2351－2362.

[6] PLUMB O A, SPOLEK G A, OLMSTEAD B A. Heat and mass transfer in wood during drying[J]. **Int J Heat Mass Transfer**, 1985, **28**(9): 1669－1678.

（渠　源　编辑）

水平直管道中气体—颗粒两相流实验研究= **An Experimental Study of Gas-granule Two-phase Flows in a Horizontal Straight Pipeline** [刊, 汉] / XUE Yuan, YAO Qiang, ZHANG Jin-cheng (Department of Thermal Energy Engineering, Tsinghua University, Beijing, China, Post Code: 100084) // Journal of Engineering for Thermal Energy & Power. — 2003, 18(1). —39 ~42, 49

The flow field of gas-granule two-phase flows was measured by using a laser technique. During a test with the help of a three-dimensional particle dynamics analyzer measurements were taken of the hourly average speed of glass micro-pearls consisting of 0 - 100 μm granules and a pulse speed distribution with the volume fraction of the granule phase being between 10^{-4} and 10^{-5}. The test results indicate that even for granules with a diameter less than 100 μm their existence in the gas-phase flow field will still give rise to a change in turbulent flow field structure. It has also been observed during the test that the turbulent-flow intensity of gas-granule two-phase flows will increase with the decrease in granule diameter. Furthermore, regarding the distribution of pulsation speed the characteristics of pulsation and random distribution can be observed in the neighborhood of tube wall surfaces. **Key words**: gas-granule two-phase flow, turbulent flow, particle dynamic analyzer

加热上升管内相及相界面密度径向分布特性实验研究= **An Experimental Study on the Characteristics of Phase and Interphase-density Radial Profile in a Heated Riser Tube** [刊, 汉] / SUN Qi, YANG Rui-chang (Thermal Energy Engineering Department, Tsinghua University, Beijing, China, Post Code: 100084), ZHAO Hua (National Key Laboratory of Bubble Physics and Natural Circulation under the China National Nuclear Power Research and Design Academy, Chengdu, China, Post Code: 610041) // Journal of Engineering for Thermal Energy &Power. — 2003, 18 (1). —43 ~46

With the help of a dual-sensor optical probe measured and studied were the radial profile characteristics of both the void fraction of steam-water dual-phase flow and the interphase density in a heated riser tube. On the basis of test results the basic law of the phase and interphase density radial-profile was investigated. Through the investigation it is found that the void fraction of the two-phase flow in the heated riser tube exhibits in the radial direction a non-uniform distribution. Depending on different operating conditions, the void fraction distribution on the whole diameter may assume an approximate U-shape, saddle shape, or an approximate arc shape with a central zone located higher than a near-wall zone. The interphase density along the whole diameter features an approximate U-shaped distribution. **Key words**: two-phase flow, void fraction, interphase density, optical probe

新型不锈钢波纹管性能及强化传热的实验研究= **An Experimental Study of the Performance of Novel Stainless Steel-made Corrugated Tubes and Their Intensified Heat Transfer** [刊, 汉] / TAN Yu-fei, CHEN Jia-xin (Electromechanical College under the Harbin Institute of Technology, Harbin, China, Post Code: 150090) // Journal of Engineering for Thermal Energy &Power. — 2003, 18(1). —47 ~49

Corrugated tubes made of a new type of stainless steel are multi-layer ones fabricated by the use of a special technique involving a concave wave formation process. In-tube flows are of an equal-diameter flow cluster type and arc-shaped flow cluster type, which can introduce a periodic change of flow speed and pressure. With the production of an intensive perturbation between cold and hot fluids a compound intensified heat exchange is realized. The corrugated tubes were tested for their pressure-bearing capacity and an experimental study of intensified heat exchange law was performed under water-water heat exchange conditions. The intensified heat exchange mechanism of the corrugated tubes was analyzed and an applicable range of optimized dimensions determined for the tubes, thus providing a theoretical basis for the use of corrugated tube-based heat exchangers. **Key words**: corrugated tube made of a new type of stainless steel, experimental study, intensified heat transfer

薄层毛细多孔介质湿区干燥过程相变传热传质常压模型= **Phase-transformation Heat Transfer and Mass Transfer Constant-pressure Model for the Drying Process of a Thin-layer Capillary Porous Media Wet-region** [刊, 汉] / LU Tao, SHEN Sheng-qiang (Power Engineering Department, Dalian University of Scien e &Technology,

Dalian, China, Post Code: 116024) // Journal of Engineering for Thermal Energy & Power. — 2003, 18(1). —50 ~ 52, 77

With a liquid-phase residual saturation degree Sir being assigned a definition a wet capillary porous media drying-zone is divided into a wet zone and a dry one. On this basis set up was a phase-transformation heat transfer and mass transfer constant-pressure model for the drying process of a wet region with liquid-phase saturation-degree S and temperature T serving as parameters. By using a full-hidden finite difference method a numerical calculation was conducted of the above-cited model. The numerical solution indicates that with the help of the model one can accurately forecast the change of the liquid-phase saturation-degree S and temperature T in the drying process of the wet region. **Key words**: capillary porous media, phase transformation, heat transfer and mass transfer

电磁式在线自动平衡系统及其动平衡方法研究= **The Study of An On-line Automatic Dynamic Balancing System and Its Dynamic Balancing Method When Used on a Flexible Rotor** [刊, 汉] / WANG Xi-xuan, ZENG Sheng (Chemical Machinery Research Institute under the Zhejiang University, Hangzhou, China, Post Code: 310027) // Journal of Engineering for Thermal Energy & Power. — 2003, 18(1). —53 ~ 57

An innovative on-line automatic dynamic balancing system is proposed along with a description of its working principle, construction and dynamic balancing method. The system is equipped with one or more than one automatic dynamic balancing head on the shaft of a rotating machine. The stator of the balancing head is capable of producing a non-contact electromagnetic force to drive the balancing disc installed on a rotating shaft. Each balancing head has two or three balancing discs, each of which has been provided with a balancing block (or called the balancing mass). The total balancing vector as a resultant composed of the balancing masses of the two or three balancing discs can balance the loss of balance of the rotor. The vibration of the shaft and positioning of the balancing discs can be detected by relevant sensors. The balancing disc assumes a single-direction movement mode, which can considerably simplify a control system. The movement principle and procedures of the balancing disc aimed at a dynamic balancing of the rotor are also discussed. The dynamic balancing test has been successfully conducted on an experimental test rig incorporating a flexible rotor. **Key words**: automatic dynamic balancing, on-line dynamic balancing, electromagnetic balancing head

基于免疫进化算法的过热汽温自整定 PID 控制研究= **A Study of the Immune Evolutionary Algorithm-based Self-tuning PID Control of Superheated Steam Temperature** [刊, 汉] / TAN Ying-zi (Automation Department, Southeastern University, Nanjing, China, Post Code: 210096), SHEN Jiong, LU Zhen-zhong (Power Engineering Department, Southeastern University, Nanjing, China, Post Code: 210096) // Journal of Engineering for Thermal Energy & Power. — 2003, 18(1). —58 ~ 62

In accordance with biological immune-system characteristics the authors have come up with a method of self-tuning PID controller parameters on the basis of an immune evolutionary algorithm. The immune evolutionary algorithm has introduced memory cells and features diversity and an anti-body concentration regulation mechanism, ensuring a rapid and stable convergence to attain an overall optimal point. A simulation of the superheated steam temperature control system has demonstrated the validity of the recommended algorithm. **Key words**: immune evolutionary algorithm, PID parameter self-tuning, superheated steam temperature control

火电厂耐热钢承压部件的蠕变损伤研究= **A Study of the Creep-related Damage of Heat-resistant Steel Pressure Parts of a Thermal Power Plant** [刊, 汉] / GUO Jing (Institute of Power & Mechanical Engineering under the Wuhan University, Wuhan, China, Post Code: 430072), ZHAN Ping (Institute of Urban Construction under the Wuhan University, Wuhan, China, Post Code: 430072), WANG Wen-an (Institute of Civil Engineering under the Wuhan University, Wuhan, China, Post Code: 430072) // Journal of Engineering for Thermal Energy & Power. — 2003, 18(1). —63 ~ 66

Heat-resistant steel materials are often used for the pressure parts and components of a thermal power plant, such as steam pipelines. After being subjected to high-temperatures and high-pressures lasting for a long time and with the even-